arXiv:physics/0509265v2 [physics.atom-ph] 16 Nov 2005

Nuclear Charge Radii of ^{9,11}Li: the Influence of Halo Neutrons

R. Sánchez,[1] W. Nörtershäuser,[1,2] G. Ewald,[1] D. Albers,[3] J. Behr,[3] P. Bricault,[3] B.A. Bushaw,[4] A. Dax,[1,*] J. Dilling,[3] M. Dombsky,[3] G.W.F. Drake,[5] S. Götte,[1] R. Kirchner,[1] H.-J. Kluge,[1] Th. Kühl,[1] J. Lassen,[3] C.D.P. Levy,[3] M.R. Pearson,[3] E.J. Prime,[3] V. Ryjkov,[3] A. Wojtaszek,[1,†] Z.-C. Yan,[6] and C. Zimmermann[2]

[1] *Gesellschaft für Schwerionenforschung, 64291 Darmstadt, Germany*
[2] *Departement of Physics, University Tübingen, D-72076 Tübingen, Germany*
[3] *TRIUMF, Vancouver, BC, Canada V6T 2A3*
[4] *Pacific Northwest National Laboratory, P.O. Box 999, Richland, WA 99352, USA*
[5] *Department of Physics, University of Windsor, Windsor, Ontario, Canada, N9B 3P4*
[6] *Department of Physics, University of New Brunswick, Fredericton, New Brunswick, Canada E3B 5A3*

(Dated: February 9, 2008)

The nuclear charge radius of ^{11}Li has been determined for the first time by high precision laser spectroscopy. On-line measurements at TRIUMF-ISAC yielded a ^{7}Li − ^{11}Li isotope shift (IS) of 25 101.23(13) MHz for the Doppler-free $2s\ ^2S_{1/2} \rightarrow 3s\ ^2S_{1/2}$ transition. IS accuracy for all other bound Li isotopes was also improved. Differences from calculated mass-based IS yield values for change in charge radius along the isotope chain. The charge radius decreases monotonically from ^{6}Li to ^{9}Li, and then increases from 2.217(35) fm to 2.467(37) fm for ^{11}Li. This is compared to various models, and it is found that a combination of halo neutron correlation and intrinsic core excitation best reproduces the experimental results.

PACS numbers: 32.10.Fn, 21.10.Ft, 27.20.+n

For twenty years, halo nuclei with diffuse outer neutron distributions have been known to exist at the limits of stability for many of the lighter elements [1]. The first discovered [2] and most renowned of these is ^{11}Li with two halo neutrons; however, details of the nuclear structure and halo – core interactions are still not well understood. Nuclear forces are not strong enough to bind a neutron to ^{9}Li, nor can they bind two neutrons into a dineutron. Yet adding two neutrons to ^{9}Li leads to a bound nucleus – ^{11}Li ($T_{1/2}$ = 8.4 ms), illustrating the importance of understanding the interaction that allow formation of the halo structure. Recent measurement [3] of the *rms* nuclear charge radius (r_c) for the two-neutron halo ^{6}He indicates that its halo is a dineutron "orbiting" the ^{4}He core. The core is a strongly-bound α-particle and model calculations [4] estimate only a 4% increase in $r_c(\alpha)$. In contrast, the ^{9}Li-like core of ^{11}Li is 'softer' and interaction between halo neutrons and core nucleons may significantly polarize the core.

An indicator for an altered ^{9}Li core would be a change in proton distribution between ^{9}Li and ^{11}Li. This was investigated in collisions which removed a proton from a ^{11}Li projectile [5], but within the rather large uncertainty, there was no clear evidence for a change in the deduced charge radius. Also, analysis and interpretation was not straightforward because of the dependence on an assumed nuclear model. A more sensitive approach to determine the change in r_c is a measurement of the isotope shift in an atomic transition [6]. A finite nuclear charge distribution reduces electron binding energies, particularly for s-electrons that have probability of being inside the nucleus, and a change in the distribution between isotopes can be observed as shifts in electronic transition energies. In light elements, the mass-based isotope shift is much larger than the nuclear volume shift; for lithium, about 10,000 times larger. The dominant portion of the mass shift is change in reduced mass (normal mass shift), but electron correlations (specific mass shift) are also important. Recent high-precision calculations account for these correlations, as well as relativistic and QED corrections [7]. In this work we present the first measurement of the ^{11}Li isotope shift in the $2s \rightarrow 3s$ Doppler-free two-photon transition, as well as refined values for all other isotopes. These are compared with calculated mass shifts, yielding nuclear charge radii that are compared with various theoretical models and interpreted in terms of halo correlation and core polarization.

The experiment must fulfil two conditions: measure the isotope shift to an uncertainty of one part in 10^5 (10^{-10} of total transition frequency), and provide an overall efficiency sufficient to observe the resonances with production yields of $\sim 10^4$ ^{11}Li atoms/s. Moreover, the short half-life requires on-line study at the production facility. We previously reported a technique [8] to perform such measurements and used it to determine the charge radii of ^{8,9}Li produced at the GSI-UNILAC. For the experiments reported here, the apparatus was moved to the TRIUMF-ISAC facility in Vancouver, Canada where ^{11}Li is produced by a 40 µA, 500 MeV proton beam impinging on a tantalum target. ^{11}Li$^+$ ions extracted from the target (typ. 30,000/s) are implanted in a hot carbon foil where they are neutralized and released as atoms into the low-field source region of a quadrupole mass spectrometer (QMS). The neutral atoms are re-ionized via

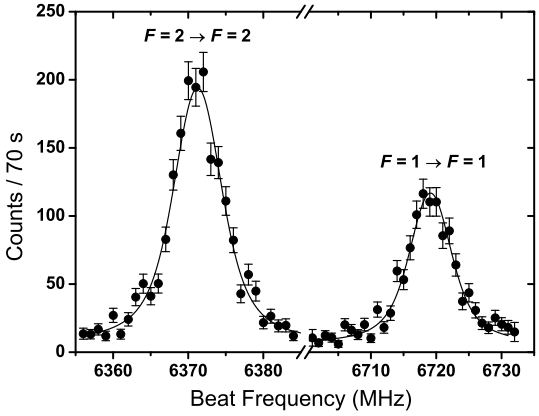

FIG. 1: Resonances in the $2s \rightarrow 3s$ transition of ^{11}Li as a function of the beat frequency between the titanium-sapphire laser and the reference diode laser. Error bars are simple counting statistics on the number of observed ion counts.

doubly-resonant four-photon ionization:

$$2s \xrightarrow{2\times 735\text{nm}} 3s \xrightarrow[30\text{ns}]{\text{decay}} 2p \xrightarrow{610\text{nm}} 3d \xrightarrow{610,735\text{nm}} \text{Li}^+ \ , \quad (1)$$

with excitation taking place at the center of a doubly-resonant optical enhancement cavity ($\sim$100$\times$) built around the QMS source region. The titanium-sapphire laser that excites the $2s \rightarrow 3s$ two-photon transition is beat-frequency servo-locked to an I_2 hyperfine line stabilized diode laser. As previously described [8], measurements on ^{11}Li (and the other isotopes) were interspersed with measurements on ^{6}Li which served as the experimental reference, and measured optical powers were used to correct for calibrated AC-Stark shifts.

Figure 1 shows a typical ^{11}Li spectrum. Twenty-four such spectra were obtained over six days of beam time. With nuclear spin $I = 3/2$, the $^2S_{1/2}$ states have $F = 1,\ 2$ hyperfine components, which obey the two-photon selection rule $\Delta F = 0$ for an $s \rightarrow s$ transition. All Li isotopes have nuclear spin and exhibit similar doublets: Isotope shifts are taken with respect to center-of-gravities of the two hyperfine lines for each isotope. Results for all isotopes, relative to ^{7}Li, are given in Table I. Values for ^{6,8,9}Li are in good agreement with our previous measurements [8], but with improved precision. The ^{6}Li isotope shift was also determined earlier with a different technique as -11 453 734(30) kHz [9]; this is significantly different from our current measurements ($\sim$ 5 times the combined uncertainties), and is attributed to unaccounted systematic errors in the prior interferometric measurements [9], as compared to the current frequency-based measurements. The IS for the halo nucleus ^{11}Li is a first-time measurement.

Successful determination of changes in r_c from the isotope shift measurements depends critically on the combined accuracy of theory and experiment. On the theoretical side, the quantum mechanical many-body problem must be solved to high accuracy in the nonrelativistic limit, and then the effects of relativity and quantum electrodynamics are included with perturbation theory. In the past, theoretical results with laser-spectroscopic accuracy were not available for atoms more complicated than helium, even in the nonrelativistic limit. This problem is now solved by variational methods involving correlated basis sets with multiple distance scales [6]. The resulting electron wave functions are used to calculate the various contributions to the mass shift, listed for ^{7,11}Li in Table II. A recent first calculation [7] of the mass polarization correction to the Bethe logarithm part of the electron self-energy has significantly reduced uncertainty in the QED contribution; overall calculation uncertainty is now limited by the relativistic recoil term of order $\alpha^2(\mu/M)$.

The total in Table II is the calculated mass-based component of the isotope shift; corresponding shifts for all isotopes are obtained directly from coefficients given in Table III of Ref. [7] and are listed in Table I. Differences from measured isotope shifts are then attributed to the nuclear volume effect and are related to r_c of the two

TABLE I: Isotope shifts measured at TRIUMF (this work) and GSI [8] [avg = weighted mean] compared with theoretical mass shifts for $^7\text{Li} - {}^A\text{Li}$ in the $2s\ ^2S_{1/2} \rightarrow 3s\ ^2S_{1/2}$ transition. Uncertainties for r_c are dominated by uncertainty in the reference radius $r_c(^7\text{Li}) = 2.39(3)$ fm [11].

Isotope		Isotope Shift, kHz	Mass Shift, kHz	r_c , fm
^{6}Li	this	−11 453 984(20)		
	GSI	−11 453 950(130)		
	avg	−11 453 983(20)	−11 453 010(56)	2.517(30)
^{8}Li	this	8 635 781(46)		
	GSI	8 635 790(150)		
	avg	8 635 782(44)	8 635 113(42)	2.299(32)
^{9}Li	this	15 333 279(40)		
	GSI	15 333 140(180)		
	avg	15 333 272(39)	15 332 025(75)	2.217(35)
^{11}Li	this	25 101 226(125)[a]	25 101 812(123)	2.467(37)

[a] 68 kHz statistical + 57 kHz systematic from AC-Stark shift

TABLE II: Contributions to the $^7\text{Li} - {}^{11}\text{Li}$ mass shift in the $2s\ ^2S_{1/2} \rightarrow 3s\ ^2S_{1/2}$ transition, excluding nuclear size effects. μ/M is the ratio of the reduced mass and the atomic mass. Uncertainty in the nonrelativistic (μ/M) term is from uncertainty in the ^{11}Li mass [10], while limiting uncertainty in the relativistic and QED terms is computational.

Contribution (order)	kHz
Nonrelativistic (μ/M)	25 104 483 (20)
Nonrelativistic $(\mu/M)^2$	−2 968 (0)
Relativistic $\alpha^2(\mu/M)$	417 (121)
QED $\alpha^3(\mu/M)$	−120 (6)
Total	25 101 812 (123)

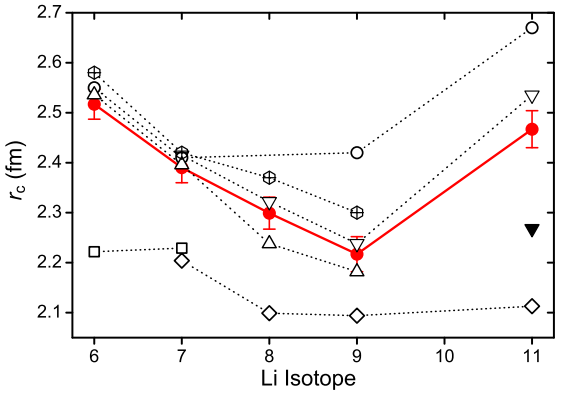

FIG. 2: (Color online) Experimental charge radii of lithium isotopes (●) compared with theoretical predictions: △: Greens-Function Monte Carlo Calculations [4, 15], ▽: Stochastic Variational Multi-Cluster Model [16, 17] (▼: assuming a frozen ^{9}Li core), ⊕: Fermionic Molecular Dynamics [18], ○: Dynamic Correlation Model [19], □ and ◇: ab-initio No-Core Shell Model [20, 21].

isotopes by

$$\delta\nu^{A,7}_{\mathrm{IS,exp}} - \delta\nu^{A,7}_{\mathrm{IS,MS}} = \frac{Ze^2}{3\hbar}\left[r_c^2(^A\mathrm{Li}) - r_c^2(^7\mathrm{Li})\right]\left(\langle\delta(r_i)\rangle_{3s} - \langle\delta(r_i)\rangle_{2s}\right) = -1.5661\frac{\mathrm{MHz}}{\mathrm{fm}^2}\left[r_c^2(^A\mathrm{Li}) - r_c^2(^7\mathrm{Li})\right] \ , \quad (2)$$

where Ze is the nuclear charge and $\langle\delta(r_i)\rangle$ are expectation values for electron density at the nucleus in the respective states [6].

Optical isotope shift measurements provide only the change in the *rms* nuclear charge radius between two isotopes. Absolute charge radii r_c must be referenced to at least one isotope that is determined with a different technique. For the stable ^{6,7}Li isotopes, r_c have been determined by elastic electron scattering [11], from which we use $r_c(^7\mathrm{Li}) = 2.39(3)$ fm as a reference radius. This and the measured ^{6,7}Li isotope shift yields $r_c(^6\mathrm{Li}) = 2.52(3)$ fm, in good agreement with the electron scattering result of 2.55(4) fm [11]. Combining measured isotope shifts, calculated mass shifts, and the ^{7}Li reference radius yields r_c for the other isotopes, as given in the last column of Table I.

The derived nuclear charge radii are shown as filled circles in Fig. 2: while r_c decreases continuously from ^{6}Li to ^{9}Li, there is a large increase from ^{9}Li to ^{11}Li. The significance of these results becomes evident when compared with predictions from different nuclear models, also shown in Fig. 2. Models using point-proton radii r_{pp} are converted to nuclear charge radii r_c by folding in proton [12] and neutron [13] mean-square charge radii:

$$\langle r_c^2\rangle = \langle r_{pp}^2\rangle + \langle R_p^2\rangle + \frac{N}{Z}\langle R_n^2\rangle + \frac{3\hbar^2}{4m_p^2c^2} \ , \quad (3)$$

where the last term is the Darwin-Foldy correction for "Zitterbewegung" of the proton [14].

Neither conventional shell model nor self-consistent Hartree-Fock calculations have correctly reproduced halo-specific anomalous properties of light nuclei close to the neutron drip-line. Early models for ^{11}Li only treated its three-body character, without considering possible polarization of the ^{9}Li core [22]; thus, change in nuclear charge radius could only be caused by correlation of the two halo neutrons. If they spend most of their time on the same side of the core, the center-of-mass (CM) is clearly different from the core center, the ^{9}Li core orbits the CM, and the averaged charge distribution is diffused. Forssén *et al.* [23] constructed corresponding wave functions for ^{11}Li to obtain an analytical model for electromagnetic dissociation of halo nuclei. The ^{11}Li *rms* matter radius of 3.55 fm was adjusted to be in good agreement with experiment [24]; the predicted CM - core distance R_{CM} ranged from 0.8 fm to 1.08 fm. The approximation [25] $r_c(^{11}\mathrm{Li}) = \left[R_{\mathrm{CM}}^2 + r_c^2(^9\mathrm{Li})\right]^{1/2} = 2.40(6)$ fm is in reasonable agreement with, but slightly lower than, our experimental result. However, information available on the binary neutron-^{9}Li (core) interaction is insufficient for these calculations to yield structural details on ^{11}Li, nor do they make predictions for changes in r_c between the non-halo nuclei.

The dynamic correlation model (DCM) is a more advanced scheme that starts from shell model states, and then introduces neutron-core interaction with a two-body potential [19, 26]. This leads to an admixture of virtually excited single-particle states from the core. For ^{11}Li, excited bound and continuum states of ^{9}Li up to 50 MeV were included in the analysis. Charge radii calculated (○ in Fig. 2) for ^{6,7}Li agree well with our measurements, and while those for ^{9,11}Li are clearly overestimated, the increase from ^{9}Li to ^{11}Li is correctly reflected.

More sophisticated nuclear models treat interactions between individual nucleons using realistic nucleon-nucleon (*NN*) and three-nucleon (*NNN*) interactions. *NN* potentials are usually based on the multi-energy partial-wave analysis of elastic *NN* scattering data produced by the Nijmegen group [27] in 1993, while the *NNN* interaction parameters are adjusted to fit the binding energies of light nuclei. Greens-Function Monte-Carlo (GFMC) calculations [4, 15], the most fundamental description available for light nuclei, have been completed for most nuclei with mass numbers $A \leq 12$. Results for the isotopes ^{6,7,8,9}Li are shown (△) in Fig. 2 and are in good agreement with the experimental results. The general trend is reproduced, but thus far the model has not been able to reproduce the ^{11}Li binding energy.

No-Core Shell Model (NCSM) calculations have been performed using realistic *NN* potentials. Earlier calculations [21] (◇) for ^{7,8,9,11}Li treated three-body interactions as an effective phenomenological potential, while recent

work [20] (□) included microscopic three-body potentials and was applied to ^{6,7}Li. As seen in Fig. 2, neither the absolute charge radii, nor the trend along the isotopic chain are in agreement with our results.

The Fermionic Molecular Dynamics (FMD) model [28] uses Gaussian wave packets for individual nucleons. The *NN*-interaction is derived from the Argonne V18 interaction, treating short-range correlations explicitly with a unitary operator. Predictions of the model [18] (⊕) are in good agreement with experiment for ^{6,7,8,9}Li, but, like GFMC, the halo structure of ^{11}Li has not yet been successfully modelled.

Calculations that consider interactions between all individual nucleons quickly become very complex and time consuming with increasing nucleon number. Cluster models like the stochastic variational multi-cluster (SVMC) calculations of Varga *et al.* [16, 17] freeze some parts of the model space and allow focus on those degrees of freedom thought to be most relevant to the physical behaviour of a given nucleus. To a large extent, this cluster structure can also be identified in FMD calculations. The building blocks in the SVMC model are the nucleons p and n, the α-particle, and the tritium nucleus t. The nuclei α and t are not treated as structureless particles; their wave functions are constructed on the nucleonic level and only nucleon motion within the clusters is approximated by simple shell-model configurations. The many-body state then describes the correlated relative motion of the different clusters in a fully anti-symmetrized wave function that obeys the Pauli principle and thus also accounts for correlated motion of the halo neutrons. The nucleon-nucleon interactions are chosen to reproduce, *e.g.*, phase shifts in *NN*, αN and $\alpha\alpha$ scattering, and deuteron size and binding energy. Additional effective nucleon-nucleon interactions are included to account for three-nucleon interactions. This model clearly shows the best agreement with our experiment (▽ in Fig. 2). Calculations for ^{11}Li were performed both with and without possible excitations of the ^{9}Li core by the halo neutrons. Including these intrinsic excitations results in $r_{\rm c}(^{11}{\rm Li}) = 2.52$ fm, in good agreement with experiment, while neglecting them results in the much smaller value $r_{\rm c}(^{11}{\rm Li}) = 2.28$ fm (▼ in Fig. 2). Thus, within the framework of SVMC, neutron correlations alone cannot reproduce the large change in $r_{\rm c}$ between ^{9}Li and ^{11}Li observed in the experiment. The calculations rather indicate that the core is indeed perturbed and that this perturbation accounts for most of the charge radius increase. It will be interesting to see whether the model is also able to describe correlations in the momentum distributions of breakup fragments [29]. We also note that while the SVMC model clearly shows the best agreement with our measured nuclear charge radii, it's predictions for nuclear electromagnetic moments [17] still have significant discrepancies from experimental values, indicating that further work is still needed.

This work is supported from BMBF contract No. 06TU203. Support from the U.S. DOE Office of Science (B.A.B.), NRC through TRIUMF, NSERC and SHARCnet (G.W.F.D. and Z.-C.Y.) is acknowledged. A.W. was supported by a Marie-Curie Fellowship of the European Community Programme IHP under contract number HPMT-CT-2000-00197. We thank the target laboratory at GSI for providing the carbon foil catcher, Nikolaus Kurz, Mohammad Al-Turany (GSI) and the ISAC computer division at TRIUMF for support in data acquisition, Melvin Good for help during installation of the experiment at TRIUMF, and René Roy for providing a liquid scintillator.

* Current address CERN, CH-1211 Geneva 23, Switzerland.
† Current address Institute of Physics, Swietokrzyska Academy, PL-25-406, Kielce, Poland.

[1] A. S. Jensen *et al.*, Rev. Mod. Phys. **76**, 215 (2004).
[2] I. Tanihata *et al.*, Phys. Rev. Lett. **55**, 2676 (1985).
[3] L.-B. Wang *et al.*, Phys. Rev. Lett. **93**, 142501 (2004).
[4] S. C. Pieper and R. B. Wiringa, Annual Rev. Nucl. Part. Science **51**, 53 (2001).
[5] B. Blank *et al.*, Z. Phys. A **343**, 375 (1992).
[6] Z.-C. Yan and G. W. F. Drake, Phys. Rev. A **61**, 022504 (2000).
[7] Z.-C. Yan and G. W. F. Drake, Phys. Rev. Lett. **91**, 113004 (2003).
[8] G. Ewald *et al.*, Phys. Rev. Lett. **93**, 113002 (2004).
[9] B. A. Bushaw *et al.*, Phys. Rev. Lett. **91**, 043004 (2003).
[10] C. Bachelet *et al.*, Eur. Phys. J. A **25 Supp. 1**, 31 (2005).
[11] C. W. de Jager, H. deVries, and C. deVries, At. Data Nucl. Data Tables **14**, 479 (1974).
[12] I. Sick, Phys. Rev. Lett. B **576**, 62 (2003).
[13] S. Kopecky *et al.*, Phys. Rev. C **56**, 2229 (1997).
[14] J. L. Friar, J. Martorell, and D. W. L. Sprung, Phys. Rev. A **56**, 4579 (1997).
[15] S.C. Pieper, K. Varga and R.B. Wiringa, Phys. Rev. C **66**, 044310 (2002).
[16] K. Varga, Y. Suzuki, and I. Tanihata, Phys. Rev. C **52**, 3013 (1995).
[17] K. Varga, Y. Suzuki, and R. G. Lovas, Phys. Rev. C **66**, 041302 (2002).
[18] T. Neff, H. Feldmeier, and R. Roth, in 21. Winter workshop on Nuclear Dynamics, Breckenridge, Colorado, USA, (2005).
[19] M. Tomaselli *et al.*, Nucl. Phys. A **690**, 298c (2001).
[20] P. Navrátil and W. E. Ormand, Phys. Rev. C **68**, 034305 (2003).
[21] P. Navrátil and B. R. Barrett, Phys. Rev. C **57**, 3119 (1998).
[22] M. V. Zhukov *et al.*, Phys. Rep. **231**, 151 (1993).
[23] C. Forssén, V. D. Efros, and M. V. Zhukov, Nucl. Phys. A **706**, 48 (2002).
[24] P. Egelhof *et al.*, Eur. Phys. J. A 15 27 (2002).
[25] M. V. Zhukov, Chalmers University of Technology, (2005).
[26] K. E. Lassila *et al.*, Phys. Rev. **126**, 881 (1962).
[27] V. G. J. Stoks *et al.*, Phys. Rev. C **48**, 792 (1993).

[28] T. Neff, H. Feldmeier, and R. Roth, Nucl. Phys. A **752**, 321 (2005).

[29] H. Simon *et al.*, Phys. Rev. Lett. **83**, 496 (1999).